Laser Characteristics for VCSELs for 77 K and 4 K Optical Data Applications

Mina Bayat and Dennis G. Deppe, *Fellow, IEEE*

***Abstract*— Small-sized vertical-cavity surface-emitting laser (VCSEL) offer the possibility of very low power consumption along with high reliability for cryogenic data transfer. Cryogenic data transfer has applications in focal plane array cameras operating at 77 K, and at the lower temperature of 4 K for data extraction from superconducting circuits. A theoretical analysis is presented for 77 K and 4 K operation based on small cavity, oxide-free VCSEL sizes of 2 to 6 μm, that have been shown to operate efficiently at room temperature. Temperature dependent operation for optimally-designed VCSELs are studied by calculating the response of the laser at 77 K and 4 K to estimate their bias conditions needed to reach modulation speed for cryogenic optical links. The temperature influence is to decrease threshold for reducing temperature, and to increase differential gain for reducing temperature. The two effects predict very low bias currents for small cavity VCSELs to reach needed data speed for cryogenic optical data links. Changing the number of top-mirror pairs has also been studied to determine how cavity design impacts speed and bit energy. Our design and performance predictions paves the way for realizing highly efficient, ultra-small VCSEL arrays with applications in optical interconnects.**

***Index Terms*—Vertical cavity surface emitting lasers, high speed modulation, laser physics, semiconductor devices, optical data transmission.**

I. INTRODUCTION

There are growing applications for which high efficiency optical data transfer is needed from cryogenic environments into room temperature data output. These include focal plane arrays [1]–[2], operating at 77 K and superconducting circuits that operate at 4 K [3], [4]. Achieving high efficiency at the cryogenic temperatures is a key challenge, because of the necessity to reduce heating in the cryogenic environment [3], [5]. The optical data transfer can be accomplished using a free space interconnect, using an optical window, or through one or more optical fibers [6].

Vertical-cavity surface-emitting lasers (VCSELs) could provide a very efficient, low cost and compact solution for these cryogenic optical data links [7], [8]. However, oxide VCSELs [7]–[14] suffer internal stress due to the oxide, that is known to cause early VCSEL failure, and could be problematic for cryogenic operation.

D.G. Deppe is with sdPhotonics and College of Optics & Photonics, University of Central Florida, Orlando, FL 32186 USA (e-mail: ddeppe@sdphotonics.com).

M. Bayat is with College of Optics & Photonics, University of Central Florida, Orlando, FL 32186 USA.

To counter these problems in oxide VCSELs, oxide-free VCSELs have recently been developed that can be scaled to micro-meter size with record efficiency [15]–[21].

These small cavity oxide-free VCSELs can operate at high efficiency and present a low bit energy solution to optical data transfer. The VCSEL's high efficiency coupling to optical fiber and direct modulation reduce or eliminate optical scattering loss that accompanies modulator approaches. The VCSEL is also expected to be a much lower cost for an overall solution to cryogenic data links than modulator approaches that include multiple fibers in and out of a cryogenic system, and a tunable laser outside the cryostat for the low power modulators such as microdisks.

Laser diode simulations that include temperature dependent gain distributions analyzed using the electronic density of states of the gain region and coupling to the VCSEL cavity modes are applied to these small cavity VCSELs to analyze their expected low temperature operation for optimized devices. Here we make projections of key VCSELs properties using an analysis based on the temperature-dependent threshold and differential gain for 4 K and 77 K operation.

The key to the low bit energy potential is the laser cavity scaling and temperature influence on the VCSEL lasing threshold and differential gain. For optimal design the VCSEL threshold scales with reducing temperature as ~ $k_{\mathrm{B}}T$, where $\mathrm{k_B}$ is Boltzman's constant and T is temperature. The differential gain scales as $1/(k_{\mathrm{B}}T)$. Threshold also ideally scales with reducing aperture size πr_{A}^2 as long as laser efficiency is maintained, where r_{A} is the aperture radius, and lateral diffusion of carriers under the current aperture can be greatly reduced. The combined effects indicate that when properly designed, directly modulated VCSELs present a very high efficiency path for optical data interconnects used to extract data from cryogenic systems.

The projection from the model suggests that high-speed modulation can be achieved at 4 K at just few μAs of bias current, with optimized 77 K devices requiring approximately 10 μA of current for 2 μm diameter cavity size demonstrated to reach high efficiency at room temperature [15]. The extremely low bias current predicts very low bit energy and high efficiency at the cryogenic operation, and make the oxide-free VCSEL an important route for cryogenic optical interconnects.

II. INTRINSIC MODULATION MODEL

Previously we have reported a model of the intrinsic modulation response that incorporates temperature dependent carrier distributions and temperature dependent cavity detuning

relative to the laser's gain spectrum [22]. We employed laser rate equations as the start point to model the temperature dependence of the small cavity lasers as given in [22]. This analysis included bulk electronic states of the gain region that could become populated when internal self-heating led to thermal rollover [22]. As shown in Eqs. (1) and (2), the rate equations for photon number and for the number of electrons and holes in the gain region can be written as

$$\frac{dn_m(t,T_J)}{dt} = -\frac{\omega_{c,m}}{Q_m}(T_J)n_m(t,T_J) + g_{st,m}(N_e,T_J)n_m(t,T_J) + g_{sp,m}(N_e,T_J) \quad (1)$$

$$\frac{dN_e(t,T_J)}{dt} = \frac{I(t)}{q} - \sum_m [g_{st,m}(N_e,T_J)n_m(t,T_J) + g_{sp,m}(N_e,T_J)] \quad (2)$$

where n_m is the photon number of the m-th mode in the cavity, Q_m is the quality factor, q is the charge of an electron, and $\omega_{c,m}$ is the lasing frequency in the cavity. N_e is the number of electrons in the active region, I is the bias current injected into the active region. $g_{st,m}$ is the gain coefficient related to stimulated emission, and $g_{sp,m}$ is the spontaneous emission coefficient. All terms in Eqs. (1) and (2) are function of the junction temperature T_J. We assume charge neutrality in the quantum well gain region that includes the thermal populations in the bulk states of the gain region so

$$N_e(t,T_J) = N_h(t,T_J) \quad (3)$$

where N_h is the number of holes in the active region. Therefore, the modulation of the holes is the same as the modulation of the electrons.

The analysis becomes simplified for cryogenic operation since bias currents can be much lower, and electron-hole populations are confined mainly to the quantum well electronic states. The intrinsic modulation response is expressed as a transfer function of the photon density over electron density in frequency domain. By using small signal response analysis and applying Fourier transform to the rate equations in time domain, we can find the expression for the frequency response. Eq. (4) shows the expression for the intrinsic modulation response, derived from semiconductor rate equations,

$$H_I(\omega) = \frac{\frac{\omega_c}{Q}(T)\Delta n(\omega,T)}{\frac{\Delta I(\omega)}{q}} \approx \frac{\frac{\omega_c}{Q}(T)G_{Diff}(T)n_0(T)}{-\omega^2 - i\omega G_{Diff}(T)n_0(T) + \frac{\omega_c}{Q}(T)G_{Diff}(T)n_0(T)} \quad (4)$$

where $n_0(T)$ is the photon number and can be obtained by solving the rate equations. G_{Diff} in (5) is differential gain, which is a function of junction temperature and electron numbers (N_e). It can be found by solving the rate equations in steady state,

$$G_{Diff}(T_J) = \frac{dg_{st}}{dN_e}(T_J) \quad (5)$$

The output power of the laser is related to photon numbers by the following expression:

$$P_{out} = \frac{\omega_c}{Q}\eta_{diff}\hbar\omega_c n \quad (6)$$

where η_{diff} is the differential slope efficiency. Below we assume that the slope efficiency is 70% based on reasonable mirror reflectivities and optical loss, but the results are not too dependent on the precise value.

III. ROOM TEMPERATURE PERFORMANCE

We have previously presented experimental results on lithographic and oxide-free VCSELs as small as 1, 2, 3 and 4 μm in diameter at room temperature [15]–[17]. The lasing characteristics, including threshold currents, maximum power, differential quantum efficiency (D.Q.E.), power conversion efficiency (P.C.E.), are shown in Table I. Accordingly, high output power, high reliability, and minimum bit energy can be achieved from these small-sized oxide-free VCSELs at room temperature.

TABLE I
Threshold current, maximum power, differential quantum efficiency (DQE) and power conversion efficiency (PCE) for oxide-free VCSELs size from 1 to 4 μm.

Device Size (μm)	I_{th} (mA)	P_{max} (mW)	DQE	PCE
1	0.33	5.00	79.7%	37.4%
2	0.30	7.97	73.4%	45.5%
3	0.32	11.61	76.0%	49.0%
4	0.42	14.00	72.7%	48.5%

IV. INTRINSIC MODULATION MODEL AT CRYOGENIC

In this work we are making projections for 4 K and 77 K operation of ultra-small oxide-free VCSELs. For cryogenic operation only consider the first mode ($m = 1$). At low temperatures, the rate equations expressed by (1) and (2) can be approximated as the following:

$$\frac{dn}{dt} = -\frac{\omega_c}{Q}n + N_{QW}\Gamma G_{QW}\{\left[1 - e^{-N_e A(T)} - e^{-N_e B(T)}\right]n + \left[1 - e^{-N_e A(T)}\right]\left[1 - e^{-N_e B(T)}\right]\} \quad (7)$$

$$\frac{dN_e}{dt} = \frac{I}{q} - N_{QW}\Gamma G_{QW}\left[1 - e^{-N_e A(T)} - e^{-N_e B(T)}\right]n - \frac{N_e}{\tau_{sp}} \quad (8)$$

where

$$A(T) = \frac{\pi\hbar^2}{m_e N_{QW} A_L k_B T}$$

$$B(T) = \frac{\pi\hbar^2}{m_h N_{QW} A_L k_B T}.$$

m_e and m_h are the effective masses of electrons and holes in the quantum wells, A_L is the area of the lasing region, N_{QW} is

the number of quantum wells in the active region, Γ is the 3-dimensional confinement factor where we have assumed the transverse confinement is unity, k_B is the Boltzmann constant, and τ_{sp} is the spontaneous lifetime due to the semiconductor dipole transition, assuming a filled electron state and empty hole state. G_{QW} includes the dipole strength of the planar quantum wells, and along with constant factors is given by

$$G_{QW} = 4\pi L_x L_y q^2 \frac{\left|d_{c,v}.E^*(z_{QW})\right|^2}{3\hbar} \frac{m_r}{\pi\hbar^2} \tag{9}$$

where m_r is the reduced effective mass of an electron and hole pair, $L_x L_y$ is the lasing area of the quantum wells in x-y plane perpendicular to the direction of quantum well thickness (z), and $E(z_{QW})$ is normalized field strength that accounts for the actual confined laser field intensity in the semiconductor cavity. $qd_{c,v}$ is the dipole moment between the electron and hole in conduction and valence band and can be found from the term of interest for spontaneous emission rate in a 2-level system given by,

$$\frac{1}{\tau_{sp}} = \frac{n_r q^2 \left|d_{c,v}\right|^2 \omega_{2,1}^3}{3\pi\varepsilon_0 \hbar c^3} \tag{10}$$

so the dipole moment can be calculated from

$$\left|d_{c,v}\right|^2 = \frac{\frac{1}{\tau_{sp}} 3\pi\varepsilon_0 \hbar c^3}{q^2 n_r \omega_{2,1}^3} \tag{11}$$

where n_r is refractive index in the active region, ε_0 is vacuum permittivity and $\omega_{2,1}$ is the lasing frequency in the cavity. It can be shown that gain (g_{st}) at low temperature is expressed by,

$$g_{st} = N_{QW}\Gamma G_{QW}\left(1 - e^{-\frac{N_e\pi\hbar^2}{m_e N_{QW} A_L k_B T}} - e^{-\frac{N_e\pi\hbar^2}{m_h N_{QW} A_L k_B T}}\right) \tag{12}$$

so differential gain will be given by,

$$G_{diff} = \frac{dg_{st}}{dN_e} = \frac{\Gamma G_{QW}\pi\hbar^2}{A_L k_B T}\left(\frac{e^{-\frac{N_e\pi\hbar^2}{m_e N_{QW} A_L k_B T}}}{m_e} - \frac{e^{-\frac{N_e\pi\hbar^2}{m_h N_{QW} A_L k_B T}}}{m_h}\right) \tag{13}$$

V. DEVICE STRUCTURE

Below we consider an oxide-free VCSEL. It is a Half-wave cavity structure designed with 15 p-type AlAs/15%AlGaAs quarter-wave top mirror pairs and three GaAs quantum well and two cavity spacers around the cavity (65%AlGaAs) and completed with 35 n-type 15%AlGaAs/AlAs quarter wave bottom mirror pairs and two 15%AlGaAs layers for phase match and GaAs as the substrate. This structure is designed for an assumed lasing wavelength of 845 nm.

VI. L-I CURVE AND MODULATION RESPONSE OF THE DEVICE AT T=4 K AND T=77 K

In this section, the results of simulations are given and show the impact of temperature, device size, and cavity design on the VCSEL performance. By solving the rate equations shown in Eqs. (7) and (8) and using the parameters calculated for device structure, the number of electrons in the active region vs. bias current, L-I characteristics, and modulation speed are calculated.

Fig. 1 shows the number of electrons vs. bias current for a 2 μm oxide-free VCSEL with different number of top-mirror pairs calculated at $T = 4$ K and $T = 77$ K.

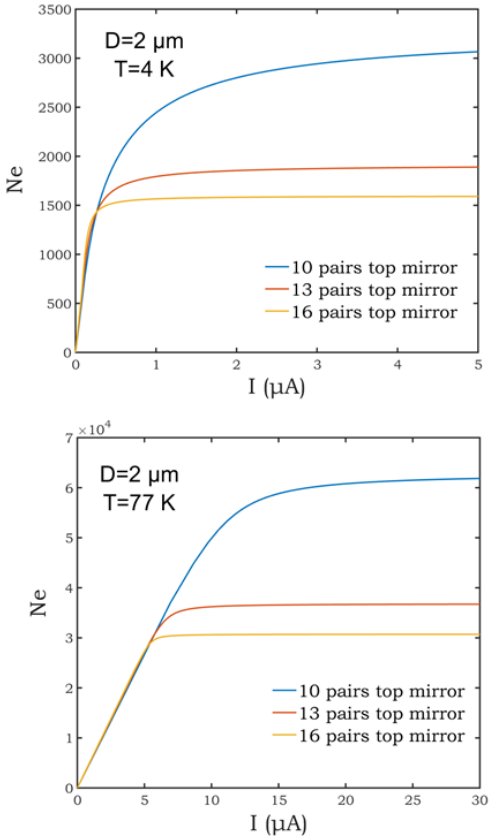

Fig. 1. Variation of the number of electrons in the active region with the bias current for a 2 μm oxide-free VCSEL lasing at 845 nm calculated at (Upper) T=4 K. (Lower) T=77 K.

As it can be seen in Fig. 1, by increasing the bias current, the number of electrons in the active region increases linearly. Once the bias current passes the threshold current, the number of electrons saturates. Also it can be observed that the higher the number top-mirror pairs, the lower the lasing bias current threshold. According to this analysis, the VCSEL with 16 top-mirror pairs leads to ~20% and ~50% lower threshold number of electrons compare to the two other VCSELs with 13 and 10 pairs top mirror.

Also at 4 K, the threshold current is predicted to be capable of reaching a value over an order of magnitude lower than that

in 77K. Therefore, the VCSEL will have novel threshold performance at lower temperatures, due to reduction of the carrier distributions in the quantum wells.

Fig. 2 shows calculated L-I characteristics of an oxide-free VCSEL with 16 top-mirror pairs for a variety of device sizes ranging from 2 μm to 6 μm in diameter at different temperatures. As shown in Fig. 2, the threshold current decreases by decreasing the device size, indicating the smaller size lithographic VCSELs have better performance. The threshold current of 2 μm device is 160 nA at 4 K and 5 μA at 77 K.

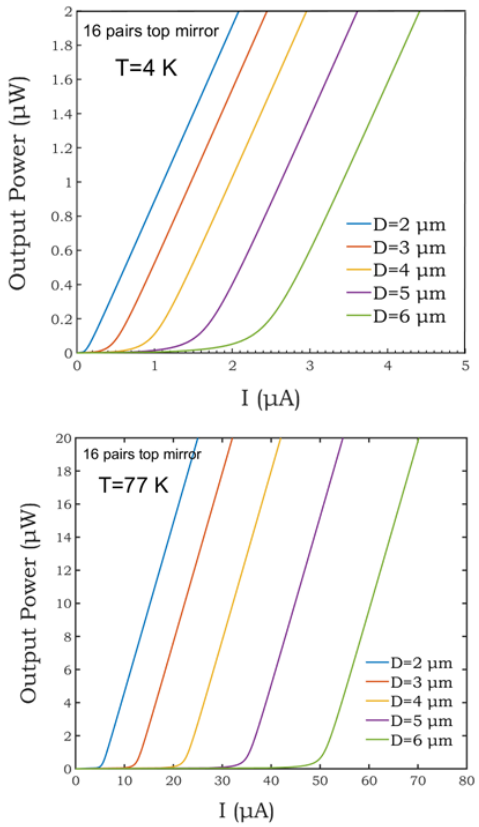

Fig. 2. Output power vs. bias current for the 2, 3, 4, 5 and 6 μm diameter oxide-free VCSEL lasing at 845 nm calculated at (Upper) *T*=4 K. (Lower) *T*=77 K.

The bias current for achieving a specific 3dB bandwidth has also been calculated to determine the impact of bias current on the intrinsic 3dB bandwidth for a number of top-mirror pairs. Fig. 3 shows the calculated results for a 2 μm diameter oxide-free VCSEL for 8, 9, 10, 11, 12 and 14 pairs of top mirrors. The analysis predicts intrinsic speed can be increased by reducing junction temperature and shrinking the laser cavity size. In addition, the reduction in thermal broadening of the electron-hole pairs confined in the quantum wells enables much lower reflectivity to be used at cryogenic temperatures than room temperature, and still achieve lasing.

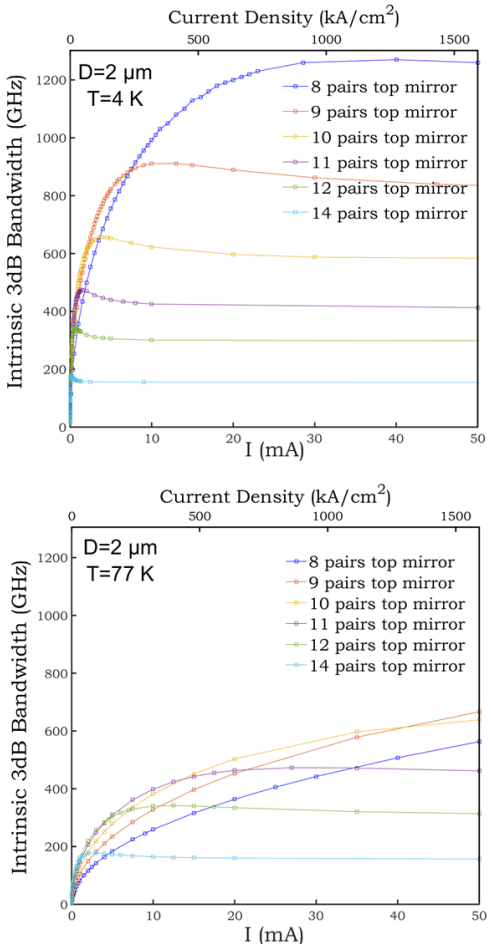

Fig. 3. 3dB bandwidth vs. current of a 2 μm oxide-free VCSEL lasing at 845 nm, with different number of top-mirror pairs calculated at (Upper) *T*=4 K. (Lower) *T*=77 K.

Fig.4 shows the analysis conducted in Fig.3 at the low current regime. From these curves the bias current can be determined to reach a given calculated modulation speed. These bias currents are predicted to be very low. For instance, the bias current required to reach 20 GHz speed is 623 nA at 4 K, and 15.1 μA at 77 K, assuming 16 pairs of top mirror.

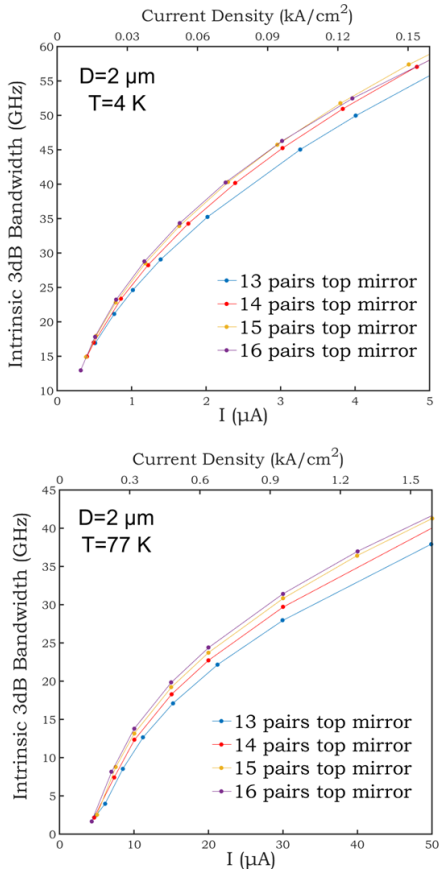

Fig. 4. 3dB bandwidth vs. current of a 2 µm oxide-free VCSEL lasing at 845 nm with different top mirror pairs calculated at (Upper) *T*=4 K. *T*=77 K (looking to low currents).

Fig. 5 shows the impact of top mirror reflectivity of the VCSEL on the lasing threshold current at temperatures of T=4 K and T=77 K. Based on this analysis, we can decide which structure will have a better performance. The mirror reflectivity increases with the number of mirror pairs, thus reducing the threshold current density. Top mirror with 16 pairs has reflectivity of 99.4% and according to the Fig. 5 it has lowest threshold current compare to other top mirror structures. It has threshold current of 0.16 µA for 4 K and 4.3 µA for 77 K. Also, the analysis shows that the lasing threshold current performance at 4 K is much better than that at 77 K.

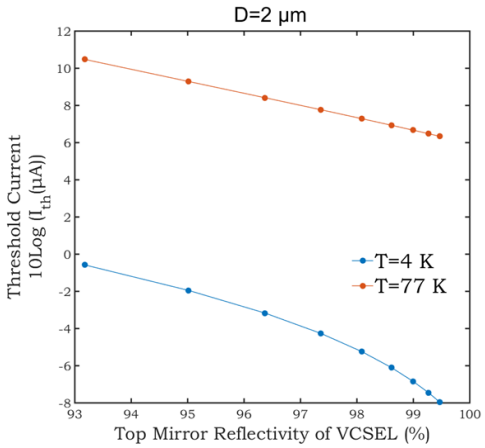

Fig. 5. Threshold Current vs. Top Mirror Reflectivity for a 2 µm oxide-free VCSEL lasing at 845 nm calculated at *T*=4 K and *T*=77 K.

Also top mirror reflectivity which is dependent on the number of top-mirror pairs has impact on the intrinsic 3-dB bandwidth of the VCSEL, as shown in Fig. 6 for a 2 µm oxide-free VCSEL at $T = 4$ K and bias current of 2.5 µA.

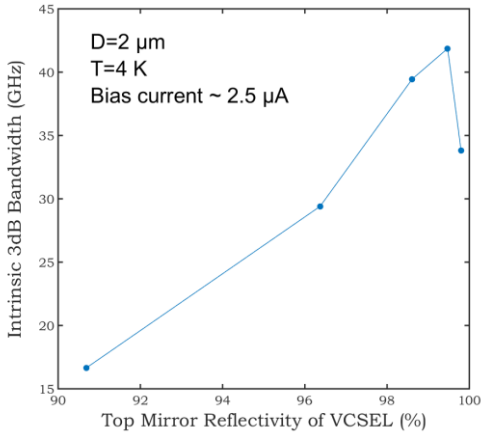

Fig. 6. Intrinsic 3 dB bandwidth vs. top mirror reflectivity for a 2 µm oxide-free VCSEL lasing at 845 nm calculated at *T*=4 K.

The intrinsic modulation response of a 2 µm oxide-free VCSEL, simulated based on Eq. (4) at T=4 K for different pairs of top mirror, is shown in Fig. 7. The 3dB bandwidth of each device can be extracted from the figure. Based on this analysis, we can make predictions about the speed of the device for different top mirrors. The device with 16 pairs of top mirror has higher 3dB bandwidth.

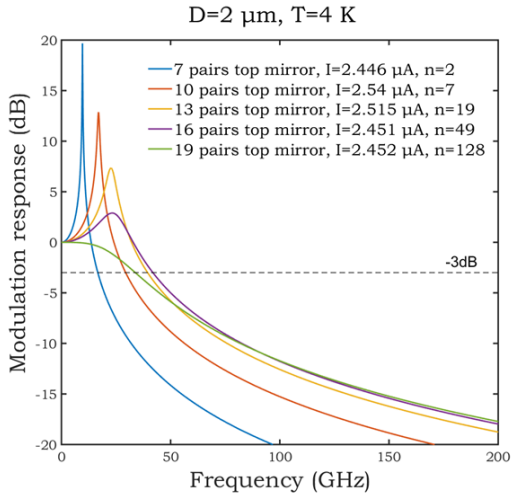

Fig. 7. Frequency response of a 2 µm oxide-free VCSEL lasing at 845 nm calculated at temperature of *T*=4 K for different number of top-mirror pairs.

Fig. 8 shows the modulation response of a 2 µm oxide-free VCSEL with 16 pairs top mirror for different bias currents at *T*=4 K. Accordingly, the bias current of 603 nA is a current needed to reach small signal intrinsic speed of 20 GHz.

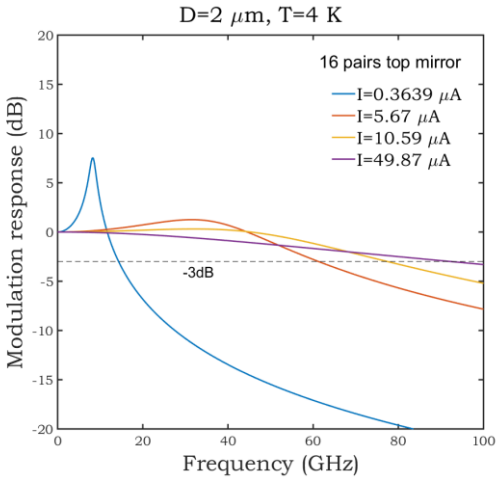

Fig. 8. Frequency response of a 2 µm oxide-free VCSEL lasing at 845 nm calculated at temperature of *T*=4 K for a 16 pairs top mirror at different bias currents.

VII. CONCLUSION

In summary, we have investigated the cryogenic operation of ultra-small oxide-free VCSELs with applications in cryogenic optical data transfer. An experimental data on lithographic oxide-free VCSELs as small as 1, 2, 3 and 4 µm in diameter at room temperature has been presented, showing high output power, high reliability and minimum bit energy. Projections have been made for key VCSELs properties at cryogenic using intrinsic-modulation-response model for oxide-free VCSEL sizes of 2 to 6 µm at 4 K and 77 K operation. Analysis indicates that the threshold current decreases significantly with reducing temperature, which makes it possible to achieve a better performance for ultra-small oxide-free VCSELs in low temperatures. Additionally, the impact of cavity design parameters such as the number of layers in top mirror on the lasing threshold is investigated.

Simulation results indicate the small size lithographic VCSELs are expected to have very low bias current, high reliability, high efficiency, and low bit energy due to size scaling of the laser at the cryogenic operation. It is shown that the 2 µm diameter oxide-free VCSEL with 16 pairs in top mirror is promising to have high intrinsic modulation bandwidth at 4 K with small threshold current compared to the ones in higher temperatures. We therefore think ultra-small oxide-free VCSEL arrays are promising platforms for future cryogenic optical interconnects.

ACKNOWLEDGEMENTS

This work has been supported in part by the Army Research Office under Grant W911NF1510579, by the Air Force Office of Sponsored Research under MURI Grant to the University of Texas at Austin, by the Army Research Laboratory under SBIR contract W911NF14C088, by the Army Research Office SBIR contract W911NF17P0048, and by IARPA under the Supercables program under award W911NF1920165.

REFERENCES

[1] P.R. Jorden *et al*., "A gigapixel commercially manufactured cryogenic camera for the J-PAS 2.5m survey telescope," in *Proc. SPIE*, vol. 8453, pp. 84530J-1–84530J-11, Sep. 2012.

[2] R. J. Dorn *et al*., "Evaluation of the Teledyne SIDECAR ASIC at cryogenic temperature using a visible hybrid H2RG focal plane array in 32 channel readout mode," in *Proc. SPIE*, vol. 7021, pp. 70210Q-1–70210Q-12, July 2008.

[3] T. Ortlepp *et al*., "Superconductor-to-semiconductor interface circuit for high data rates," *IEEE Trans. Appl. Supercond.*, vol. 19, no. 1, pp. 28–34, Feb. 2009.

[4] S. S. Tannu, D. M. Carmean, and M. K. Qureshi "Cryogenic-DRAM based memory system for scalable quantum computers: a feasibility study" *Proc. Int. Symp. on Memory Systems*, 2017, pp. 189-195.

[5] P. Figueiredo *et al*., "Progress in high-power continuous-wave quantum cascade lasers [Invited]," *Appl. Opt.*, vol. 56, no. 31, pp. H15–H23, Nov. 2017.

[6] S. S. Polkoo and C. K. Renshaw, "Imaging-based beam steering for free-space optical communication," *Appl. Opt.*, vol. 58, no. 13, pp. D12-D21, May 2019.

[7] D. L. Huffaker, D. G. Deppe, K. Kumar, and T. J. Rogers, "Native-oxide defined ring contact for low-threshold vertical-cavity lasers," *Appl. Phys. Lett.*, vol. 65, pp. 97-99, July 1994.

[8] J. M. Dallesasse and D. G. Deppe, "III–V oxidation: Discoveries and applications in vertical-cavity surface-emitting lasers," *Proc. IEEE*, vol. 101, no. 10, pp. 2234–2242, Oct. 2013.

[9] G. M. Yang, M. H. MacDougal, and P. D. Dapkus, "Ultralow threshold current vertical-cavity surface-emitting lasers obtained with selective oxidation," *Electron. Lett.*, vol. 31, no. 11, pp. 886–888, May 1995.

[10] D. L. Huffaker and D. G. Deppe, "Intracavity contacts for low-threshold oxide-confined vertical-cavity surface-emitting lasers," *IEEE Photon. Technol. Lett.*, vol. 11, no. 8, pp. 934–936, Aug. 1999.

[11] R. Jager *et al*., "57% wallplug efficiency oxide-confined 850 nm wavelength GaAs VCSELs," *Electron. Lett.*, vol. 33, no. 4, pp. 330–331, Feb. 1997.

[12] N. Iwai *et al*., "1060 nm VCSEL array for optical interconnection," *Furukawa Rev*., vol. 36, pp. 1–4, Mar. 2009.

[13] D. M. Kuchta *et al*., "A 50 Gb/s NRZ modulated 850 nm VCSEL transmitter operating error free to 90 °C," *J. Lightw. Technol.*, vol. 33, no. 4, pp. 802–810, Feb. 2015.

[14] D. M. Kuchta *et al*., "A 71-Gb/s NRZ modulated 850-nm VCSEL-based optical link," IEEE Photon. Technol. Lett., vol. 27, no. 6, pp. 577–580, Mar. 2015.

[15] X. Yang *et al*., "Small-sized lithographic single-mode VCSELs with high-power conversion efficiency," in *Proc. SPIE*, vol. 9381, pp. 93810R-1–93810R-6, Mar. 2015.

[16] D. G. Deppe *et al*., "Letting the heat out: Integration of VCSELs with Si," in *Proc. IEEE Opt. Interconnects Conf.*, Coronado, CA, USA, May 2014.

[17] M. Li, X. Yang, N. Cox, J. Beadsworth, and D. Deppe, "Record low differential resistance using lithographic VCSELs," in *Proc. Conf. Lasers Electro-Opt.*, San Jose, CA, USA, Jun. 2016, pp. 1–2.

[18] G. Zhao *et al*., "Record low thermal resistance of mode-confined VCSELs using AlAs/AlGaAs DBRs," in *Proc. Conf. Lasers Electro-Opt.*, San Jose, CA, USA, Jun. 2013, pp. 1–2.

[19] X. Yang, G. Zhao, M. Li, and D. G. Deppe, "Stress test of lithographic vertical-cavity surface-emitting lasers under extreme operating conditions," *Electron. Lett.*, vol. 51, no. 16, pp. 1279–1280, Aug. 2015.

[20] X. Yang, M. Li, G. Zhao, S. Freisem, and D. G. Deppe, "Small oxide-free vertical-cavity surface-emitting lasers with high efficiency and high power," *Electron. Lett.*, vol. 50, no. 24, pp. 1864–1866, Nov. 2014.

[21] X. Yang, M. Li, G. Zhao, Y. Zhang, S. Freisem, and D. G. Deppe, "Oxide-free vertical-cavity surface-emitting lasers with low junction temperature and high drive level," *Electron. Lett.*, vol. 50, no. 20, pp. 1474–1475, Sep. 2014.

[22] D. G. Deppe, M. Li, X. Yang, and M. Bayat, "Advanced VCSEL technology: self–heating and intrinsic modulation response," *IEEE J. Quantum Electron.*, vol. 54, no. 3, 2400209-1–2400209-9, June 2018.

Mina Bayat was born in Zanjan, Iran. She received her B.S. (magna cum laude) degree from the University of Tabriz, Tabriz, Iran, in 2007, and the M.S. degree from Sharif University of Technology, Tehran, Iran, in 2010 both in Electrical Engineering and M.Sc. in Optics from the College of Optics & Photonics (CREOL) at the University of Central Florida, Orlando, USA, in 2015. She is currently a PhD student in optics at CREOL. Her current research interests include Fabrication, design and simulations of VCSELs and semiconductor lasers.

Dennis G. Deppe (F'00) received the B.S., M.S., and Ph.D. degrees in electrical engineering from the University of Illinois at Urbana-Champaign, Urbana, in 1981, 1985, and 1988. His Ph.D. work centered on atom diffusion in III–V semiconductor heterostructures and its use in superlattice disordering and laser fabrication.

After obtaining his Ph.D., he was employed as a Member of Technical Staff at AT&T Bell Laboratories, Murray Hill, New Jersey, where he researched and developed vertical-cavity surface-emitting lasers. In 1990, he joined the University of Texas at Austin, where he became a Professor in the Electrical and Computer Engineering Department and held the Cullen Trust Endowed Professorship in engineering. At the University of Central Florida, Orlando, he holds the Florida Photonics Center of Excellence Endowed Chair in nanophotonics. His recent research interests include optoelectronics, laser physics, epitaxial crystal growth, and quantum optics. His research has included a number of firsts, including the identification of the Si-vacancy complex as responsible for Si diffusion in GaAs and AlGaAs, the identification of the p-dopant base diffusion mechanism in III–V bipolar transistors, the first demonstration of a continuous-wave laser on Si, the first oxide-confined VCSEL, the first GaAs-based 1.3 μm quantum-dot laser diode, and the first demonstrations of high T_0 quantum-dot laser diodes.

He has authored or coauthored more than 200 journal articles and presented more than 200 conference papers in the area of III–V semiconductors.

Dr. Deppe has been awarded the Nicholas Holonyak Jr. Award from the Optical Society of America and the IEEE LEOS Engineering Achievement Award, and served as an IEEE LEOS Distinguished Lecturer. He is a Fellow of the IEEE and OSA.